



ELSEVIER

Physica C 370 (2002) 228–238

PHYSICA C

www.elsevier.com/locate/physc

# Current transport along grain boundaries in d-wave superconductors

M. Carmody<sup>a,\*</sup>, L.D. Marks<sup>b</sup>, K.L. Merkle<sup>c</sup>

<sup>a</sup> Rockwell Science Center, 1049 Camino Dos Rios, Thousand Oaks, CA 91358, USA

<sup>b</sup> Department of Materials Science and Engineering, Northwestern University, Evanston, IL 60208, USA

<sup>c</sup> Materials Science Division and Science and Technology Center for Superconductivity, Argonne National Laboratory, Argonne, IL 60439, USA

Received 29 June 2001; accepted 6 July 2001

## Abstract

The use of a classic phase retrieval algorithm has been previously used to determine the local critical current  $J_c(x)$  along the length of grain boundary Josephson junctions that can be characterized using a standard s-wave model. The phase retrieval approach has been modified for use with d-wave dominated superconductors to allow for negative local currents along the boundary. In general solutions to the 1-D phase problem are not unique, however in the present work special constraints are employed experimentally to ensure uniqueness. The various current distribution solutions and their possible uniqueness are explored. The solutions are consistent with most existing d-wave Josephson junction boundary models and can be used to understand the basic current distribution along  $45^\circ$   $\text{YBa}_2\text{Cu}_3\text{O}_{7-x}$  grain boundary junctions as well as providing a means for mapping the location of self-generated flux cores. © 2001 Published by Elsevier Science B.V.

PACS: 74.25.Fy; 74.25.Ha; 73.40.Gk

Keywords: Josephson junction; Phase retrieval; Grain boundary superconductor; YBCO

## 1. Introduction

Understanding the current transport mechanisms along the length of grain boundaries in high temperature superconductor systems is of vital interest for technological applications as well as for basic scientific investigations of superconduc-

tivity. The total critical current across a length of grain boundary is suppressed relative to the adjacent grains, thus high current transport applications such as power transmission wires are limited by the current density carrying capacity of the grain boundary. Microelectronic devices such as SQUIDS based on the Josephson effect of high angle grain boundaries are also dependent on the current transport properties across grain boundaries. The superconducting system of interest is  $\text{YBa}_2\text{Cu}_3\text{O}_{7-x}$  (YBCO) due to its high superconducting transition temperature ( $\sim 92$  K) and the

\* Corresponding author. Tel.: +1-805-373-4085; fax: +1-805-373-4137.

E-mail address: mcarmody@rws.c.com (M. Carmody).

relative ease with which high quality epitaxial films can be fabricated.

The transport properties of YBCO grain boundaries depend strongly on the orientation of the adjacent grains. For example in a typical bicrystal [001] tilt grain boundary, the total critical current  $J_c$  across the grain boundary decreases roughly exponentially, by approximately three orders of magnitude when the tilt angle is increased from 0° to 45° [1–3].

For this paper we have considered the situation of a YBCO [001] 45° tilt boundary. The 45° tilt orientation has been selected to highlight the important effect that the local boundary microstructure and the symmetry of the order parameter has on the local variation of the current. The microstructure along [001] 45° tilt grain boundaries are dominated by (100)(110) type facets along the length of the boundary [4–10]. The symmetry of the order parameter for YBCO has been shown to be at least partly of  $d_{x^2-y^2}$  type and from simple geometric arguments, assuming the symmetry of the order parameter is locked into the crystal structure of the superconductor, the d-wave component of the YBCO order parameter becomes increasingly important when the misorientation angle approaches 45° [10–14]. Fig. 1 is a schematic of the  $d_{x^2-y^2}$  order parameter symmetry and ori-

entation for an asymmetric [001] 45° tilt grain boundary. When the tilt angle is 45°, the lobe of the order parameter on one side of the boundary is aligned with the node of the order parameter on the other side of the boundary. The resulting lack of overlap of the lobes across the boundary is believed to be responsible for the reported near zero critical currents at zero applied magnetic field [10–14]. Thus, a grain boundary in a pure d-wave superconductor that maintains a 45° orientation along the length of the boundary in the form of (100)(110) type facets may have zero critical current when measured in a zero field environment [10–14].

For a Josephson junction, the critical current crossing the boundary is modulated as a function of an applied magnetic field. Specifically, the critical current as a function of an applied magnetic field can be written as the modulus of the Fourier transform of the local current density,

$$I_c(H) = \left| \int_0^W J_c(x) \exp\left(\frac{2\pi i(2\lambda_L)\mu_0 H}{\Phi_0} x\right) dx \right| \quad (1)$$

where  $J_c(x)$  is the local current density along the length of the boundary and  $H$  is the magnetic field applied perpendicular to the current bias direction. From Eq. (1) it is evident that measuring the critical current as a function of an applied magnetic field can reveal information regarding the variation of the local current distribution. For a junction in the narrow limit (when the width  $W$  is less than four times the Josephson penetration depth,  $W \leq 4\lambda_J$ ), Eq. (1) is valid and can be used to calculate the correlation function of  $I_c(H)$  which gives the spacing of the current variations [15–20]. Also, it has been shown that with the use of a phase retrieval algorithm, it is possible to restore the missing phase information and calculate  $J_c(x)$  [21–24]. In general the solutions to the 1-D phase problem are not mathematically unique, however work by Greenaway, Crimmins and Fienup showed that if the appropriate boundary constraints are used that the solutions to the 1-D phase retrieval problem are almost always unique [25–27]. When multiple solutions exist, there are typically very few solutions and most are physically similar and thus represent essentially the

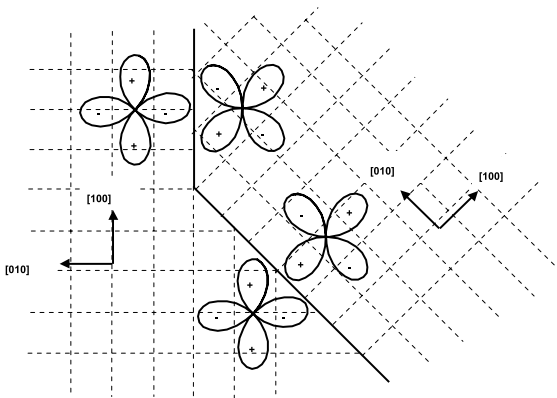


Fig. 1. Schematic of the d-wave order parameter interaction along the (100)(110) facets of a [001] 45° tilt grain boundary. Note the lobe node alignment across the boundary plane for each facet resulting in little or no overlap of the wave function for a pure d-wave superconductor with a misorientation angle of 45°.

same current distribution [21–24]. With the help of a minimization algorithm such as a genetic algorithm it is possible to find the set of all possible solutions. This technique can effectively find the local current deviations along the length of s-wave superconductor Josephson junctions. In this paper we address the issue of adapting this type of analysis to d-wave dominated superconductors.

A model proposed by Mints and Kogan suggests that the standard Fourier relation of Eq. (1) is valid for a d-wave superconductor Josephson junction [29]. The main difference that they point out is that the local critical current  $J_c(x)$  can be either positive or negative with respect to the applied current bias due to the “0” and “ $\pi$ ” facets along the boundary. Their model is consistent with existing 45° grain boundary junction  $I_c(H)$  data where the  $I_c(H)$  maximum is not at  $H = 0$  and with  $I_c(H)$  data from 45° junctions (like the junctions measured by Nicolett and Villegier) in which the diffraction pattern is near Fraunhofer despite its 45° misorientation angle [10–14,22,28].

The phase restoration algorithm that has been employed for extracting the local critical current values for s-wave Josephson junctions assumes that the local critical current is always positive. However, assuming a d-wave model identical to the one proposed by Kogan and Mints, the phase restoration approach used by Carmody et al. for restoring the local current distribution  $J(x)$  can be modified for d-wave superconductors by allowing for locally negative currents along the boundary [23,24]. The phase restoration algorithm uses a series of boundary constraints to force convergence of the current distribution solutions. For an s-wave superconductor the boundary constraints are

$$J(x) = \begin{cases} \geq 0 \\ J(x) \\ \text{real} \end{cases} \quad \text{for } |x| \leq L \quad (2)$$

where  $L$  is the length of the boundary. The only difference when applying the algorithm to a d-wave superconductor is that the requirement that  $J_c(x) \geq 0$  at all times must be relaxed to allow for negative local currents at the boundary.

## 2. Uniqueness of the 1-D phase retrieval problem

The lack of uniqueness of the 1-D phase retrieval problem has long been a source of ambiguity for physical applications of the restoration from magnitude algorithms. The basic problem can be stated as follows: Given the Fourier transform relation between  $F(u)$  and  $f(x)$  which for the continuous case can be written as

$$F(u) = \int_{-\infty}^{\infty} f(x) \exp(iux) dx \quad (3)$$

is it possible to calculate a real space object  $f(x)$  from the experimentally measured Fourier modulus  $|F(u)|$ . It is well known that the 1-D phase restoration problem can have multiple solutions and thus ambiguities in interpreting physical significance of particular solutions. Walther demonstrated that when the modulus  $|F(u)|$  is given, it is possible to multiply  $|F(u)|$  by a phase function term,

$$|F(u)| \exp(i\theta), \quad (4)$$

then by reverse Fourier transforming to generate a real space object  $f(x)$  [30]. However, Walther pointed out that any phase function  $\exp(i\theta)$  of modulus 1 arrived at randomly can be multiplied by  $|F(u)|$  and transformed to generate a real space object  $f(x)$  [30]. Thus when the only information available is the Fourier modulus  $|F(u)|$ , there can potentially exist an infinite number of solutions to the 1-D phase retrieval problem. Thus when there exists infinite ambiguity in the solutions  $f(x)$ , no relevant physical information is obtainable without additional constraints on the problem.

Walther considered the case of finite (compact) support where the function  $f(x)$  is known to be band limited to an interval  $[a,b]$  on the real  $x$ -line (Fig. 2) [30]. Fig. 3 shows a function that is band limited to the interval  $[a,b]$  where  $f(x) = 0$  everywhere outside the region  $[a,b]$ . Walther showed that when  $|F(u)|$  is multiplied by a random phase function as in Eq. (4), the resulting real space object  $f(x)$  almost never conforms to the requirement that  $f(x) = 0$  outside the interval  $[a,b]$ . Thus requiring  $f(x)$  to be zero outside a fixed interval places a severe restriction on the possible phases that can be used to generate a function  $f(x)$  that

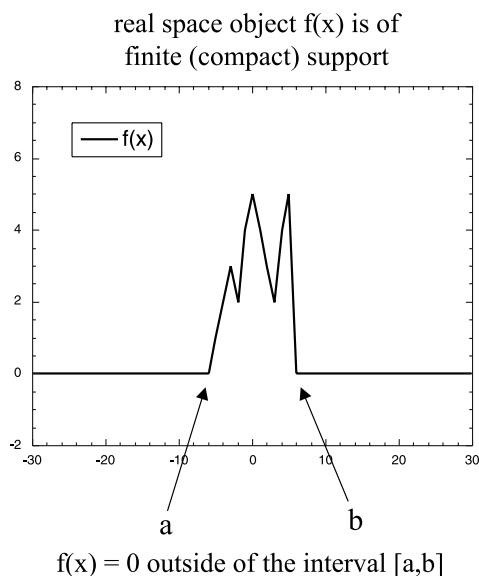


Fig. 2. Real space object  $f(x)$  of finite support (band limited) to the interval  $[a,b]$ . The finite support greatly reduces the number of possible solutions to the phase problem.

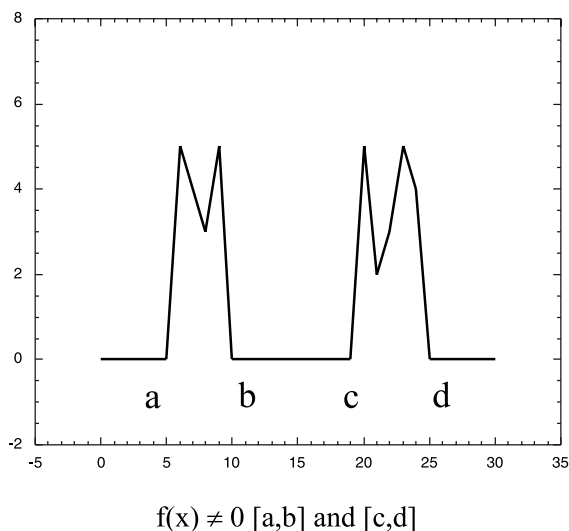


Fig. 3. Real space object  $f(x)$  with disconnected support where the object is defined to be zero outside the interval  $[a,b]$  and  $[c,d]$ . When the interval  $[b,c]$  is greater than  $[a,b]$  and  $[c,d]$  then the object  $f(x)$  is said to be of “sufficiently disconnected support” and guarantees a unique solutions to the phase problem.

conforms to the band limit  $[a,b]$ . However, the compact support requirement does not in general guarantee a unique solution. Although the possi-

ble phases have been severely restricted by the band-limit constraint, there can still exist many different solutions  $f(x)$  that when Fourier transformed have the same modulus  $|F(u)|$  [30].

Several key papers by Greenaway, Crimmins and Fienup attempted to understand the requirements for uniqueness in the 1-D phase retrieval problem and to define conditions and constraints on the real space object  $f(x)$  that would guarantee uniqueness [25–27]. Starting with the Fourier transform relationship

$$F(u) = \int_{-\infty}^{\infty} f(x) \exp(iux) dx \quad (5)$$

where  $f(x)$  is the real space object of interest.  $F(u)$  can be extended into the complex  $z$ -plane as

$$F(z) = \int_{-\infty}^{\infty} f(x) \exp(izx) dx \quad (6)$$

where  $z = u + iv$  in the complex plane.  $F(z)$  is defined as an entire function which means it is analytic over the entire  $z$ -plane. Entire functions exhibit a unique property that they may only take the value of zero ( $F(z) = 0$ ) at a set of isolated points that are unique to that function and are distributed throughout the  $z$ -plane in such a way that they tend to lie close to the real  $u$ -axis. The locations of the zero points (zeros) determine the modulus  $|F(u)|$  on the real line [25–27].

It can be shown that if there exist two functions  $F(z)$  and  $F_1(z)$  where  $|F(u)| = |F_1(u)|$ , then  $F_1(z)$  can be thought of as being derived from  $F(z)$  by the following relation

$$F_1(z) = F(z) \left( \frac{z - \bar{z}_0}{z - z_0} \right) \quad (7)$$

where  $z_0$  is a zero of  $F(z)$  and  $\bar{z}_0$  is the complex conjugate of  $z_0$ . Therefore,  $F_1(z)$  can be thought of as being derived by removing a zero at location  $z_0$  and then adding a zero at location  $\bar{z}_0$ . The zero at  $z_0$  was “flipped” or conjugated about the real line to produce a new function  $F_1(z)$  that has the same Fourier modulus  $|F(u)|$  along the real line [25–27]. Flipping any number of complex zeros about the real line will result in a new function  $F(z)$  that has the same Fourier modulus  $|F(u)|$ . Then it can be shown that a function  $F(z)$  with  $M$  complex zeros

can have  $2^M$  different unique combinations of zero flips and thus  $2^M$  different solutions to the phase problem [25–27]. Consequently, functions with no complex zeros ( $M = 0$ ) must generate only a single unique real space function  $f(x)$  since there are no complex zeros that can be flipped about the real line to produce new functions with the same modulus. Therefore, functions  $F(z)$  with only real zeros must produce unique solutions to the phase problem.

Greenaway attempted to show constraints that could be placed on the real space object  $f(x)$  that would guarantee only real zeros and thus produce a unique solution to the phase problem [25]. Greenaway argued that if a real space object  $f(x)$  had a region within the function that was equal to zero (disconnected support) then the solutions generated by phase retrieval should be unique [25]. Fig. 3 shows a function with disconnected support where the function is defined to be non-zero over the intervals  $[a,b]$  and  $[c,d]$  and defined to be zero everywhere else. Crimmins and Fienup showed that the disconnected support constraint used by Greenaway was not always unique [26,27]. They argued that the disconnected regions must be sufficiently separated to guarantee uniqueness. To ensure uniqueness, the region within the function constrained to be zero must be greater in extent than the non-zero regions. The object  $f(x)$  in Fig. 3 is a real space object with sufficiently disconnected support where region  $[b,c]$  is greater in length than region  $[a,b]$  and  $[c,d]$ . Fig. 4 shows a real space function with two zero regions within the object  $f(x)$ . The separation condition requires that region  $[b,c]$  and  $[d,e]$  to be longer than regions  $[a,b]$  or  $[c,d]$  to ensure uniqueness. Real space ob-

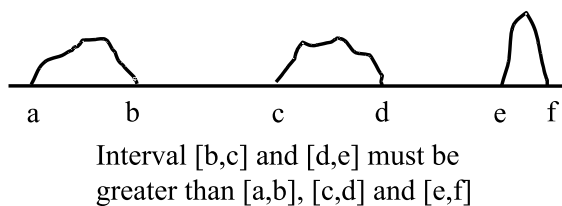


Fig. 4. Object  $f(x)$  with multiple zero intervals  $[b,c]$  and  $[d,e]$  defined to be zero each of sufficiently disconnected support such that  $[b,c]$  and  $[d,e]$  are greater in extent than both  $[a,b]$ ,  $[c,d]$  and  $[e,f]$ .

jects  $f(x)$  must be real and positive to guarantee uniqueness in all cases, however functions conforming to the separation condition that are not real or positive are “usually” unique [26,27].

Previous phase retrieval work has attempted to extract local current information from single grain boundary junctions in symmetric  $24^\circ$  tilt boundaries where the constraint that the local current must always be positive could be enforced to reduce the total number of solutions. Attempting to expand this type of analysis to  $45^\circ$  tilt boundaries is formidable since locally negative currents must be allowed for thus reducing the possibility that a unique solution to the phase problem exists. The work by Greenaway, Crimmins and Fienup demonstrated that if sufficiently disconnected support (a zero region within the boundary) can be enforced experimentally, it may be possible to obtain a unique solution to the phase problem for  $45^\circ$  grain boundaries. This paper attempts to experimentally enforce these boundary constraints along the length of a Josephson junction and use phase retrieval techniques to extract local current information from  $45^\circ$  asymmetric tilt grain boundary junctions.

### 3. Experimental techniques and results

Thin film YBCO [001] oriented asymmetric  $45^\circ$  tilt grain boundaries were fabricated using the sputter induced epitaxy technique on commercial MgO substrates [9]. Photolithography was used to pattern a microbridge across the boundary plane to ensure that each junctions conformed to the short junction limit (width  $< 4\lambda_J$ ). Starting with a single junction the samples were cooled in a magnetically shielded cryostat and critical current vs. applied magnetic flux measurements were performed with the magnetic field oriented parallel to the [001] direction of the film. The experimentally measured  $I_c(B)$  data for each  $45^\circ$  grain boundary was used in concert with the phase retrieval algorithm to calculate the local current distribution  $J(x)$  along the boundary. The details of the algorithm have been published previously, however the constraint that the local current must always be positive was relaxed to allow for locally negative

currents along 45° boundaries. The phase retrieval algorithm requires constraints on the local current  $J(x)$  to converge to a solution. For a single junction the current is constrained to be zero outside the junction length. That constraint is not sufficient to guarantee a unique solution to the phase problem, therefore a Hitachi focused ion beam (FIB) was used to etch channels along the boundary plane. The FIB etched away the YBCO leaving channels along the boundary plane that carry zero current. These zero current channels were patterned to ensure a sufficiently disconnected support constraint and thus guarantee the uniqueness of the 1-D phase retrieval algorithm.

Fig. 5 shows a SEM micrograph of a photolithographically patterned and FIB etched microbridge across a 45° boundary. The FIB etched channel is  $\approx 6 \mu\text{m}$  in width and conforms to the sufficiently disconnected support criterion that is required for uniqueness of the phase retrieval solution. Cryogenic measurements were made of the critical current as a function of an applied magnetic field. Fig. 6 shows the experimentally measured  $I_c(B)$  behavior of the junction shown in Fig. 5. The diffraction pattern is typical of many 45° grain boundary junctions where the maximum critical current is located at  $B \neq 0$ . The absence of

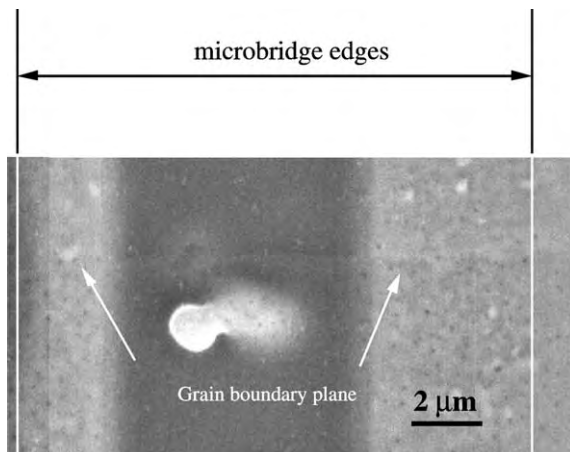


Fig. 5. SEM micrograph showing microbridge and FIB patterned region across the boundary plane. The FIB etched region is larger in extent than the adjacent grain boundary on either side of the channel and thus guarantees a sufficiently disconnected support for the phase retrieval algorithm.

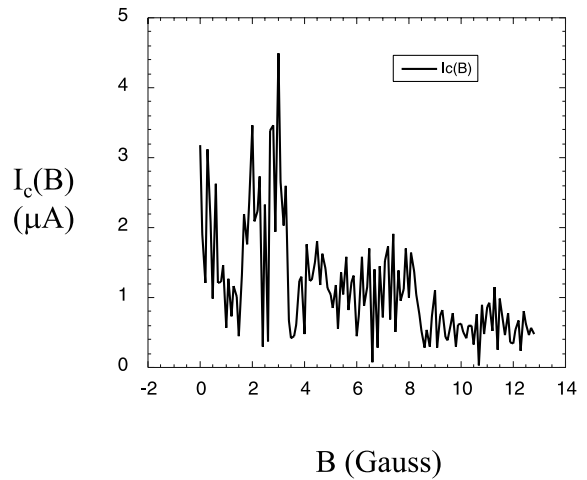


Fig. 6. Critical current vs. applied magnetic flux  $I_c(B)$  measurements for the grain boundary shown in Fig. 5 measured at 15 K. Note that the maximum current is not located at  $B = 0$ .

a large central peak is indicative of locally negative currents along the boundary. The regions etched by the FIB are evident in the photomicrograph can be assumed to carry zero current and thus can be used as a constraint in the phase retrieval algorithm. Fig. 7 shows the local current distribution

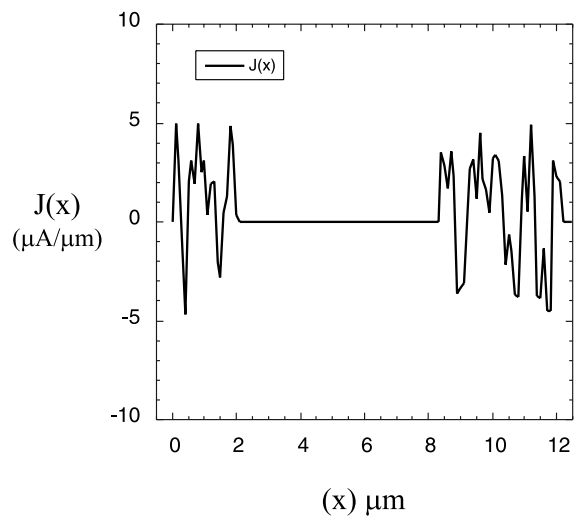


Fig. 7. Local current distribution solution  $J(x)$  along the boundary plane determined from the data in Fig. 6. Note the large local variations as well as the locally negative currents along the boundary.

$J(x)$  determined from the  $I_c(B)$  of Fig. 6. The FIB etched regions within the junction satisfies the sufficiently disconnected support constraint and thus the current distribution in Fig. 7 should be unique. Note the large variation in the local current along the length of the boundary as well as the current reversals (negative local currents) along the boundary. The Fourier relation of Eq. (1) requires locally negative currents along the boundary when the maximum current across a Josephson junction is not located at  $B = 0$ .

Fig. 8 is a SEM micrograph of a  $45^\circ$  grain boundary junction where two channels across the boundary plane have been etched with a FIB. The etched channels cannot carry current and thus act as the disconnected support for the phase retrieval algorithm, however, this particular sample does not conform to the stringent requirement of sufficiently disconnected support as put forth by Crimmins and Fienup. Fig. 9 shows the  $I_c(B)$  pattern measured from the sample in Fig. 8. Note again the large oscillations of the current and that the maximum critical current is not located at  $B = 0$ . Fig. 10 shows the current distribution solution  $J(x)$  determined from the phase retrieval technique. Only one solution was obtained to the phase retrieval problem, even though the possibility for more than one solution existed because of the lack of sufficient constraints to guarantee uniqueness.

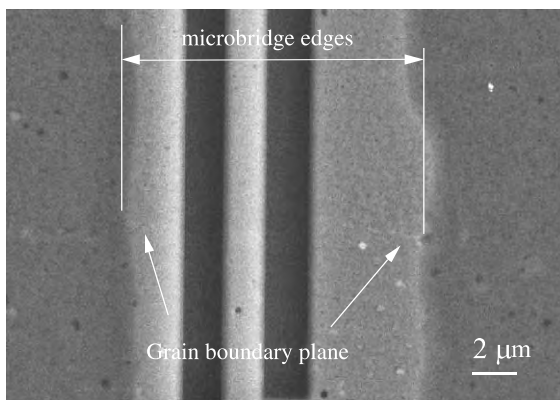


Fig. 8. SEM micrograph showing microbridge and FIB patterned regions across the boundary plane. The FIB etched regions are not larger in extent than the adjacent grain boundary on either side of the channel and thus multiple solutions may exist theoretically.

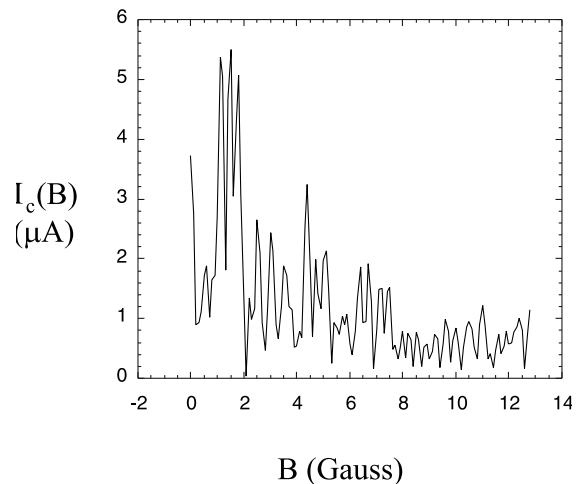


Fig. 9. Critical current vs. applied magnetic flux  $I_c(B)$  measurements for the grain boundary shown in Fig. 8 measured at 15 K. Note as in Fig. 6, the maximum critical current is not located at  $B = 0$  and thus suggests locally negative currents along the boundary plane.

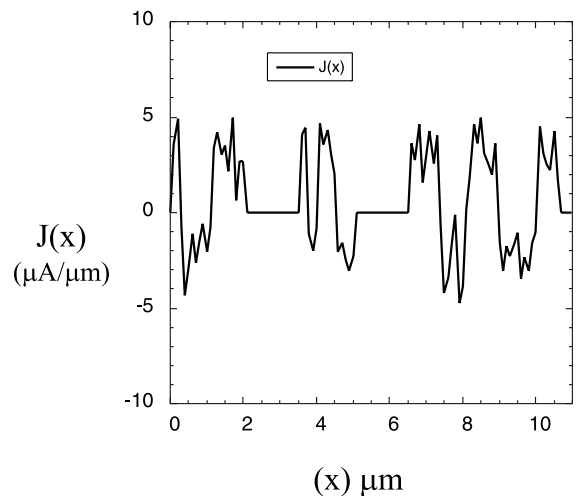


Fig. 10. Local current distribution  $J(x)$  along the boundary shown in Fig. 8. Although multiple solutions were possible, the phase retrieval algorithm in concert with a genetic algorithm was not able to find any other solutions other than mirror solutions, which are not considered “different” solutions.

Fig. 11 shows the  $I_c(B)$  behavior of a single  $45^\circ$  grain boundary junction where no channels were etched with the FIB. The single junction shows the typical  $45^\circ$  diffraction pattern with no large central current peak located at  $B = 0$ . The  $I_c(B)$  data from

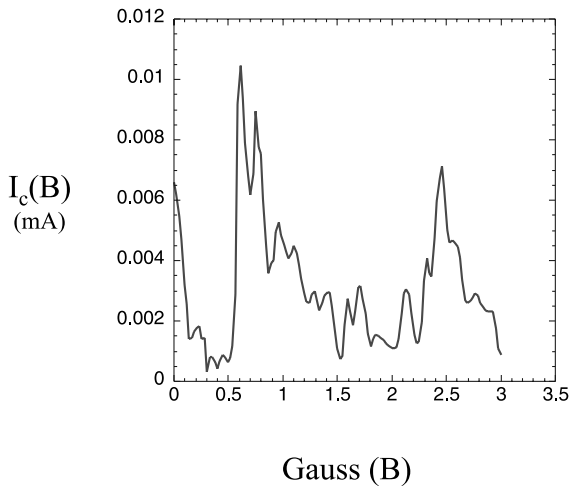


Fig. 11. Critical current vs. applied magnetic flux  $I_c(B)$  for a single  $45^\circ$  grain boundary Josephson junction. The lack of a large central current peak is typical of  $45^\circ$  junctions.

Fig. 11 was used to determine local current distributions  $J(x)$  for the junction. The junction does not have channels etched with the FIB that can be set to zero and used as a constraint to guarantee uniqueness of the solution. The constraints that can be used are the finite support of the junction (junction width is fixed and the current must be zero outside of the junction), the local current must always be less than a maximum,  $J_{c,max}$  and the total current must be positive even though locally it can be negative. Using these constraints the phase retrieval was used to calculate possible current distributions for the junction. Fig. 12 shows the different current distributions determined using the known boundary constraints and the phase retrieval algorithm. The phase retrieval algorithm was able to find several different solutions from the data in Fig. 11. The solutions are non-unique in a strict mathematical sense, but share many similar physical traits. All of the solutions share common large peaks toward the left-hand side of the solutions. Peaks largely correspond to peaks and troughs correspond to trough thus representing similar current distributions. Some of the smaller peaks toward the right side of the distribution in Fig. 12 are out of phase and thus represent ambiguities in the physical interpretation of the current distributions. It may be

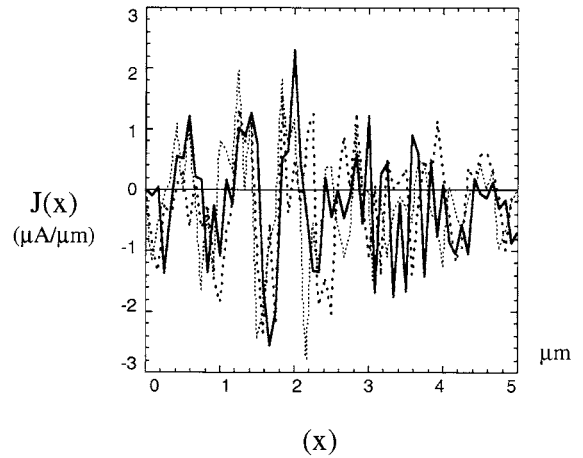


Fig. 12. Current distributions  $J(x)$  calculated from the data in Fig. 11. Multiple solutions to the phase problem exist for a single junction without disconnected support. Note the similarity between the large-scale features in the different solutions.

useful to average the various current distributions since the large peaks have a strong correlation between solutions. Fig. 13 shows the average of the three different solutions found in Fig. 12. The large-scale features common to all three solutions remain intact because of the strong correlation between solutions, however much of the fine scale

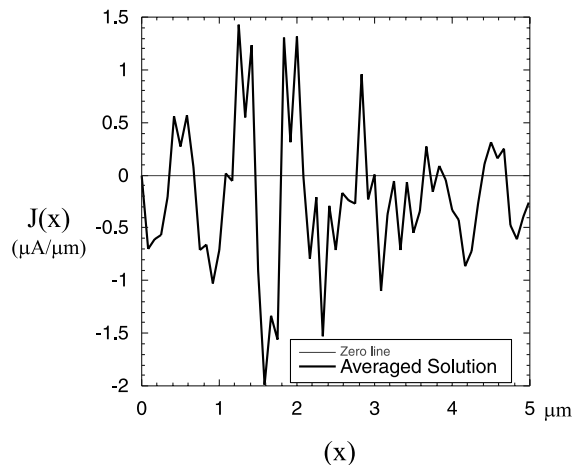


Fig. 13. Averaged solution calculated from the solutions in Fig. 12. The large-scale features have been retained in the averaged solutions because of the similarities between solutions. Some of the small-scale features have been lost or averaged out due to the various solutions being slightly out of phase.

detail is lost due to variations in the individual solutions.

#### 4. Discussion

A striking feature of all of the  $45^\circ$  grain boundary junction  $I_c(B)$  measurements is the large variations of the diffraction patterns and thus the current distribution from junction to junction. Fig. 5 is a typical critical current vs. applied magnetic field measurement on a  $45^\circ$  grain boundary junction. The maximum critical current value is not at  $B = 0$  and the pattern is highly non-uniform. Models have been proposed for  $45^\circ$  grain boundary junction dominated by the d-wave symmetry of the order parameter that model the boundary as a series of  $0$  and  $\pi$  junctions where each facet of the boundary can experience a phase shift of  $\pi$  relative to the adjacent facet [10,11,29]. A consequence of this configuration is that adjacent facets can have critical currents flowing in the opposite direction of the applied current bias even at zero applied field ( $H = 0$ ) [10,11,29]. These locally negative currents are responsible for the suppressed critical currents and the spontaneously generated flux at zero applied magnetic field [12].

Numerous studies have focused on understanding the underlying causes for these variations in current transport with increasing misorientation of the boundary plane. Grain boundary models involving a regular array of dislocations at the grain boundary have been proposed that qualitatively describe the decrease in  $J_c$  for low angles, however, these basic models do not apply to the high angle regime [31–35]. Variations in the oxygen content at the grain boundary relative to the adjacent grain and variations in the oxygen content along the length of a grain boundary also suggests locally varying current transport capabilities of the grain boundary [36–48]. Also, the orientation of the grain boundary plane relative to the adjacent crystals varies along the length of the boundary. The macroscopic misorientation angle of the superconducting grain boundary is controlled by the misorientation angle of the bicrystal substrate. However, the local orientation of the superconducting grain boundary varies greatly due

to the meandering of the grain boundary. The boundary meandering is accommodated by facets that form along the length of the junction. For  $45^\circ$   $[001]$  tilt boundaries, the microstructure is dominated by  $(100)(110)$  type facets along the length of the boundary resulting in a stair case structure (see Fig. 14). The local current can theoretically vary at the same length scale of the facets (hundreds of nanometers) due to variations in the carrier concentration along sections of the boundary. Also, it is believed that changes in the facet geometry that result in a reversal of symmetry of the order parameter manifest as a  $\pi$  phase shift and thus are responsible for the areas along the boundary with locally negative currents [11–24,29]. The boundary schematic in Fig. 14 starting from the left side shows a series of long  $(110)(100)$  type facets separated by small  $45^\circ$  steps along  $(100)(110)$  type planes. At location (A) in Fig. 11 the orientation of the long straight facets change from  $(110)(100)$  to  $(100)(110)$ . This reversal at location (A) is the type of reversal believed to be responsible for a  $\pi$  phase shift that can result in the reversal of the current direction at point (A). Consequently, not all adjacent  $(100)(110)$  type facets have a  $\pi$  phase shift associated with the interaction of the order parameter across the grain boundary plane, rather only those changes in boundary orientation that result in the

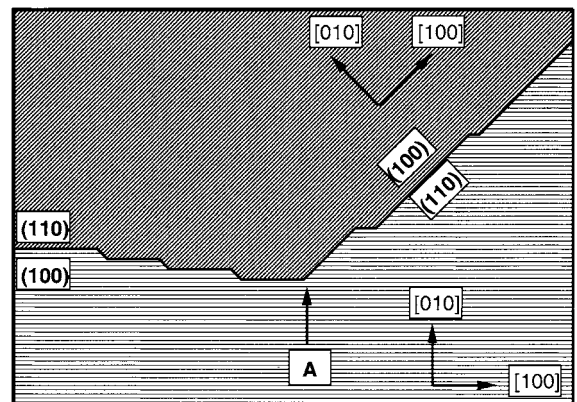


Fig. 14. Schematic of the  $(100)(110)$  type facets along the length of the grain boundary for a YBCO  $45^\circ$  tilt grain boundary. Note the symmetry reversal of the long facets at location (A).

reversal of symmetry of the long facets such as at location (A) in Fig. 11.

The local current distributions of the 45° grain boundaries from Figs. 7 and 10 demonstrate the variability from one junction to another fabricated under identical processing parameters. The phase retrieval method is capable of determining on the submicron length scale variations of  $J(x)$  along the boundary as well as the location of self-generated flux cores at current reversal centers. Scanning SQUID microscopy studies have been able to locate and confirm the presence of these self-generated flux fields for long 45° grain boundary Josephson junctions, but the resolution of these scanning techniques are not adequate for the narrow junction regime length scales [12]. Theoretical predictions based on geometric arguments for 45° grain boundaries suggest that the locally alternating current between positive and negative should vary at the same length scale as the facets. Therefore, for a typical 2  $\mu\text{m}$  wide junction, there should exist approximately 2–10 vortices of self-generated flux due to current reversals. The nature, size and distribution of these vortices for large junctions has been considered, but it is not clear as to the nature or distribution for the narrow junction limit. The phase retrieval method thus far has the greatest potential for mapping the small-scale (submicron) distribution of these currents and self-generated flux.

The resolution of the phase retrieval technique is limited by  $H_{c1}$  and the geometry of the microbridge used to isolate the junction under consideration due to possible flux-focusing effects. The ultimate resolution of the phase retrieval technique is not clear because of the junction bridge geometry, flux-focusing issues, self-generated flux along the boundary and ringing effects due to the discrete Fourier transform. However, it seems clear that real space information in the range of 0.05–0.1  $\mu\text{m}$  is clearly demonstrated to be consistent with existing d-wave models.

## 5. Conclusions

The phase retrieval technique used to analyze standard s-wave superconductors can be modified

to accommodate alternating currents in d-wave dominated superconductors. The uniqueness problem of the 1-D phase retrieval approach can be eliminated by patterning regions within the boundary plane that carry zero current and thus can be used as additional constraints to the problem. Current distributions for [001] YBCO 45° grain boundary junctions determined from critical current vs. applied magnetic field measurements show large-scale oscillations along the length of the boundary with locally alternating currents resulting in self-generated flux along the boundary. The current distributions for the 45° grain boundary junctions are consistent with existing d-wave models as well as microfilamentary models that suggest significant variations in the local current.

## Acknowledgements

This work was supported by the National Science and Foundation Office of Science and Technology Centers, under contract no. DMR 91-20000 (MC and LDM) and the United States Department of Energy, Basic Energy Sciences-Materials Science, under contract no. W-31-109-ENG-38 (KLM) and National Science Foundation grant no. DMR-9214505.

## References

- [1] D. Dimos, P. Chaudhari, J. Mannhart, F.K. LeGoues, *Phys. Rev. Lett.* 61 (1988) 219.
- [2] D. Dimos, P. Chaudhari, J. Mannhart, *Phys. Rev. B* 41 (1990) 4038.
- [3] Z.G. Ivano, P.A. Nilsson, D. Winkler, J.A. Alarco, T. Claeson, E.A. Stepansov, A.Ya. Tzalenchuk, *Appl. Phys. Lett.* 56 (1991) 3030.
- [4] J.A. Alarco, E. Olsson, Z.G. Ivanov, P.A. Nilsson, D. Winkler, E.A. Stepansov, A.Y. Tzalenchuk, *Ultramicroscopy* 51 (1993) 239.
- [5] C. Traeholt, J.G. Wen, H.W. Zandbergen, Y. Shen, J.W.M. Hilgenkamp, *Physica C* 230 (1994) 424.
- [6] I.F. Tsu, J.L. Wang, D.L. Kaiser, S.E. Babcock, *Physica C* 306 (1998) 163.
- [7] J.W. Seo, B. Kabius, U. Dahne, A. Scholen, K. Urban, *Physica C* 245 (1995) 25.
- [8] B. Kabius, J.W. Seo, T. Amrein, U. Dahne, A. Scholen, M. Siegel, K. Urban, L. Schulz, *Physica C* 231 (1994) 123.

- [9] B.V. Vuchic, K.L. Merkle, P.M. Baldo, K.A. Dean, D.B. Buchholz, R.P.H. Chang, H. Zhang, L.D. Marks, *Physica C* 270 (1996) 75.
- [10] C.A. Copetti, F. Ruders, B. Oelze, Ch. Buchal, B. Kabius, J.W. Seo, *Physica C* 253 (1995) 63.
- [11] H. Hilgenkamp, J. Mannhart, B. Mayer, *Phys. Rev. B* 53 (1996) 14586.
- [12] J. Mannhart, H. Hilgenkamp, B. Mayer, Ch. Gerber, J.R. Kirtley, K.A. Moler, M. Sigrist, *Phys. Rev. Lett.* 77 (1996) 2782.
- [13] J. Mannhart, H. Hilgenkamp, *Physica C* 317–318 (1999) 383.
- [14] J. Mannhart, B. Mayer, H. Hilgenkamp, *Z. Phys. B* 101 (1996) 175.
- [15] O.M. Froehlich, H. Schulze, A. Beck, B. Mayer, L. Alff, R. Gross, R.P. Huebener, *Appl. Phys. Lett.* 66 (1995) 2289.
- [16] S. Schuster, R. Gross, B. Mayer, R.P. Huebener, *Phys. Rev. B* 48 (1993) 16172.
- [17] X. Xiu, Q. Lu, S. Wang, Y. Dai, G. Xiong, G. Lian, R. Me, S. Wang, Z. Gan, *Physica C* 282–287 (1997) 2409.
- [18] O.M. Froehlich, H. Schulze, A. Beck, R. Gerdemann, B. Mayer, R. Gross, R.P. Huebener, *IEEE Trans. Appl. Supercond.* 5 (1995) 2188.
- [19] L. Alff, B. Mayer, S. Schuster, O. Frohlich, R. Gerdemann, A. Beck, R. Gross, *J. Appl. Phys.* 75 (1994) 1843.
- [20] A. Beck, A. Stenzel, O.M. Froehlich, R. Gerber, R. Gerdemann, L. Alff, B. Mayer, R. Gross, *IEEE Trans. Appl. Supercond.* 5 (1996) 2192.
- [21] O. Neshier, E.N. Ribak, *Appl. Phys. Lett.* 71 (1997) 1249.
- [22] M. Carmody, E. Landree, L.D. Marks, K.L. Merkle, *Physica C* 315 (1999) 145.
- [23] M. Carmody, B.H. Moeckly, K.L. Merkle, L.D. Marks, *J. Appl. Phys.* 87 (2000) 2454.
- [24] M. Carmody, K.L. Merkle, Y. Huang, L.D. Marks, B.H. Moeckly, *Interf. Sci.* 8 (2000) 231.
- [25] A.H. Greenaway, *Opt. Lett.* 1 (1977) 10.
- [26] T.R. Crimmins, J.R. Fienup, *J. Opt. Soc. Am.* 71 (1981) 1026.
- [27] T.R. Crimmins, J.R. Fienup, *J. Opt. Soc. Am.* 73 (1983) 218.
- [28] S. Nicoletti, J.C. Villegier, *J. Appl. Phys.* 82 (1997) 303.
- [29] R.G. Mints, V.G. Kogan, *Phys. Rev. B* 55 (1997) R8682.
- [30] A. Walther, *Opt. Acta* 10 (1964) 119.
- [31] M.F. Chisholm, D.A. Smith, *Phil. Mag.* 59 (1989) 181.
- [32] Y. Gao, K.L. Merkle, G. Bai, H.L.M. Chang, D.J. Lam, *Physica C* 174 (1991) 1.
- [33] N.D. Browning, J.P. Buban, P.D. Nellist, D.P. Norton, M.F. Chisholm, S.J. Pennycook, *Physica C* 294 (1998) 183.
- [34] S.E. Babcock, D.C. Larbalestier, *J. Mater. Res.* 5 (1990) 919.
- [35] M.F. Chisholm, S.J. Pennycook, *Nature* 351 (1991) 47.
- [36] S.E. Babcock, D.C. Larbalestier, *J. Phys. Chem. Solids* 55 (1994) 1125.
- [37] S.E. Babcock, J.L. Vargas, *Rev. Mater. Sci.* 25 (1995) 193.
- [38] V.P. Dravid, H. Zhang, Y.Y. Wang, *Physica C* 213 (1993) 353.
- [39] S.E. Babcock, D.C. Larbalestier, *Appl. Phys. Lett.* 55 (1989) 393.
- [40] N.D. Browning, M.F. Chisholm, S.J. Pennycook, D.P. Norton, D.H. Lowndes, *Physica C* 212 (1993) 185.
- [41] Y. Zhu, M. Suenaga, *Physica C* 252 (1995) 117.
- [42] Y. Zhu, J.M. Zua, A.R. Moodenbaugh, M. Suenaga, *Phil. Mag. A* 70 (1994) 969.
- [43] B.H. Moeckly, R.A. Buhrman, *Appl. Phys. Lett.* 65 (1994) 3126.
- [44] B.H. Moeckly, R.A. Buhrman, *IEEE Trans. Appl. Supercond.* 5 (1995) 3414.
- [45] B.H. Moeckly, D.K. Lathrop, R.A. Buhrman, *Phys. Rev. B* 47 (1993) 400.
- [46] E.A. Early, R.S. Steiner, A.F. Clark, *Phys. Rev. B* 50 (1994) 9409.
- [47] E. Sarnelli, *Interf. Sci.* 1 (1993) 287.
- [48] E. Sarnelli, P. Chaudhari, J. Lacey, *Appl. Phys. Lett.* 62 (1993) 777.